*GEOLOGICA CARPATHICA, 54, 6, BRATISLAVA, DECEMBER 2003*
*367–375*

# ALPINE LOW-GRADE METAMORPHISM OF THE PERMIAN-TRIASSIC SEDIMENTARY ROCKS FROM THE VEPORIC SUPERUNIT, WESTERN CARPATHIANS: PHYLLOSILICATE COMPOSITION AND “CRYSTALLINITY” DATA

BRANISLAV LUPTÁK[1], MARIAN JANÁK[1], DUŠAN PLAŠIENKA[1*] and SUSANNE TH. SCHMIDT[2]

[1]Geological Institute, Slovak Academy of Sciences, Dúbravská cesta 9, 840 05 Bratislava 45, Slovak Republic; branislav.luptak@savba.sk; geolmjan@savba.sk
[2]Département de Minéralogie, Rue des Maraîchers 13, 1211 Genève 4, Switzerland

*Present address: Department of Geology and Paleontology, Faculty of Natural Sciences, Comenius University Mlynská dolina, 842 15 Bratislava, Slovak Republic; plasienka@fns.uniba.sk

*(Manuscript received December 10, 2002; accepted in revised form June 23, 2003)*

**Abstract:** Alpine low-grade metamorphism related to Cretaceous orogeny has been investigated in the metasediments of the Permian-Triassic cover in the Veporic Superunit, Western Carpathians. Metaclastic rocks and marbles show metamorphic grade of upper anchizonal to epizonal (greenschist facies) conditions according to the illite “crystallinity” measurements. The chlorite thermometry of Cathelineau (1988) and Jowett (1991) yields a temperature of ca. 310–330 °C in the northern part and ca. 335–380 °C in the central and eastern parts of the Veporic Superunit. A pressure of ca. 4–4.5 kbar has been obtained from the white mica, K-feldspar and biotite-bearing rocks, supposing a temperature of ca. 380 °C. The new results suggest higher temperature and lower pressure of the Alpine low-grade metamorphism than the previous estimates. The P-T conditions of the Alpine low-grade metamorphism in the Veporic Superunit are in good agreement with the observed deformational microtextures.

**Key words:** Alpine metamorphism, Western Carpathians, Veporic Superunit, Permian-Triassic cover, geothermobarometry, “crystallinity” index.

## Introduction

Vrána (1966) presented the first important petrographical and mineralogical data on Alpine low-grade metamorphism in the Veporic Superunit of the Western Carpathians. Plašienka et al. (1989) first reported the conditions of low-grade metamorphism in Mesozoic metapelitic rocks of parautochthonous cover sequences of the Veporic Superunit based on the illite “crystallinity”. Their results prove epizonal metamorphic conditions accompanied by ductile overthrust deformations in the southern Veporic cover unit and decreasing metamorphic grade from epizonal to anchizonal conditions in the northern Veporic cover unit. No mineral chemical data have been published by the authors mentioned above. Later on, Korikovsky et al. (1992, 1997) discussed the conditions of Alpine anchimetamorphism in the Veporic Superunit.

This study presents results on Alpine metamorphism in the Veporic Superunit complementary to those reported recently by Lupták et al. (2000) and Janák et al. (2001).

The purpose of the present study is: (1) to determine the mineral parageneses and composition of individual minerals in the low-grade metasediments from the Permian-Triassic cover of the Veporic Superunit, (2) to evaluate the P-T conditions of Alpine metamorphism, and (3) to correlate these results with illite and chlorite “crystallinity”.

## Geological setting

The pre-Tertiary complexes of the Central Western Carpathians (Plašienka et al. 1997) are composed of six main Slovakocarpathian north-verging superunits: the Tatric, Veporic and Gemeric thick-skinned basement/cover nappe stacks and the Fatric, Hronic and Silicic detachment cover nappe systems (e.g. Biely 1989; Tomek 1993; Plašienka et al. 1997). All these units originated during the Cretaceous collisional shortening and stacking of the lower plate following the closure of the Meliatic Ocean during the Late Jurassic and they may be well correlated with the Austroalpine units of the Alps (Janák et al. 2001).

The Veporic Superunit (Fig. 1) is the middle of the three major, south-dipping, thick-skinned basement/cover imbricates. As a consequence of collisional thickening in the Cretaceous, the Veporic basement and its Permian-Triassic cover experienced regional Alpine metamorphism. The dominant Veporic macrostructure, a low-angle normal ductile shear zone, is interpreted as a master detachment fault, which exhumed the Veporic core by east-vergent unroofing (Plašienka et al. 1999).

The Veporic cover complexes are in marginal position on the crystalline basement or are only locally preserved in the central part. The Late Paleozoic-Mesozoic sedimentary cover

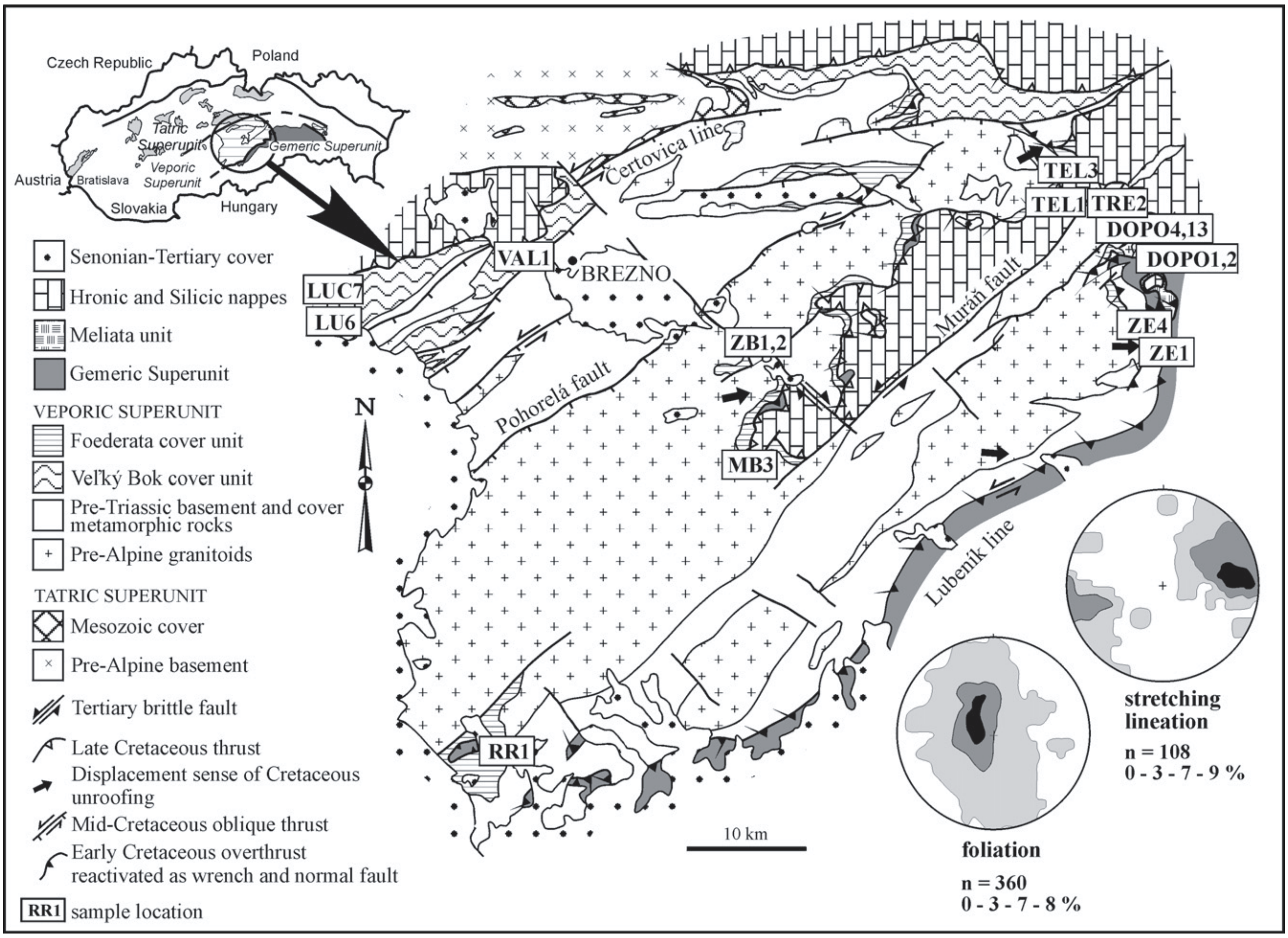

**Fig. 1.** Geological sketch map of the studied area with locations of investigated samples.

of the Veporic Superunit is subdivided into two parts — (a) the south-eastern and central Foederata Unit and (b) the northern Veľký Bok Unit.

The Foederata Unit is scarcely preserved. It consists of low- to medium-grade metamorphosed and highly foliated and deformed rocks of sedimentary origin (Plašienka et al. 1997). This unit includes Upper Permian continental clastics (metasandstones and metaconglomerates), Scythian quartzites and schists overlain by Middle to Late Triassic rocks, mostly carbonates of a passive margin environment. No Jurassic sedimentary rocks have been observed.

The Veľký Bok Unit comprises Permian red beds (Ľubietová Group, Vozárová & Vozár 1988), Scythian quartzites, Middle Triassic carbonate platform deposits, and Upper Triassic, continental Carpathian Keuper Formation. The Rhaetian and Lower Liassic littoral sedimentary rocks are superimposed by continuously deepening Upper Liassic–Lower Cretaceous deposits with typical spotted marls, nodular, cherty and siliceous limestones, radiolarites and thick Neocomian dark marly limestones, which represent the syn- and post-rift sequences (Plašienka et al. 1997).

The deformational structural association of the area covered by the Foederata Unit is dominated by a flat or moderately NE-dipping metamorphic/mylonitic foliation $S_1$, which is penetrative in both the topmost parts of the basement granitoids and in the Veporic cover units. The foliation planes show a distinct stretching lineation $L_1$ plunging generally to the east. This deformation stage $AD_1$ is completed by the moderately E- to NE-dipping shear bands, which are mesoscopically penetrative along the eastern margin of the Veporic dome (e.g. extensional crenulation cleavage — ECC, or C'-type shear bands).

Tight to isoclinal folds $F_1$ are frequent only in the Triassic marbles of the Foederata Unit, where they usually exhibit NW-verging asymmetry and axes parallel to the elongation direction. The growth of newly formed metamorphic minerals within the cover rocks is generally syn- to early post-kinematic

**Fig. 2.** Microphotographs of mineral assemblages and deformational textures in the studied rocks. **a** — Back-scattered electron (BSE) image of the metamorphosed marly limestone (LUC7). **b** — Microphotograph of metamorphosed marly limestone with chlorite rich layer (LUC7). **c** — BSE image of authigenic white micas and subhedral K-feldspars in marble (DOPO4). **d** — BSE image of biotite and phengitic white mica in Scythian schist (ZE4). **e** — Microphotograph of crenulation cleavage in the Carpathian Keuper slate (VAL1). **f** — Microphotograph of crenulation cleavage in the Scythian schist (DOPO2). **g** — Microphotograph of recrystallized quartz and white mica layers in Scythian schist (MB3). **h** — Microphotograph of chlorite porphyroblast in Scythian schist (ZE1). Wm — white mica, Phn — phengite.

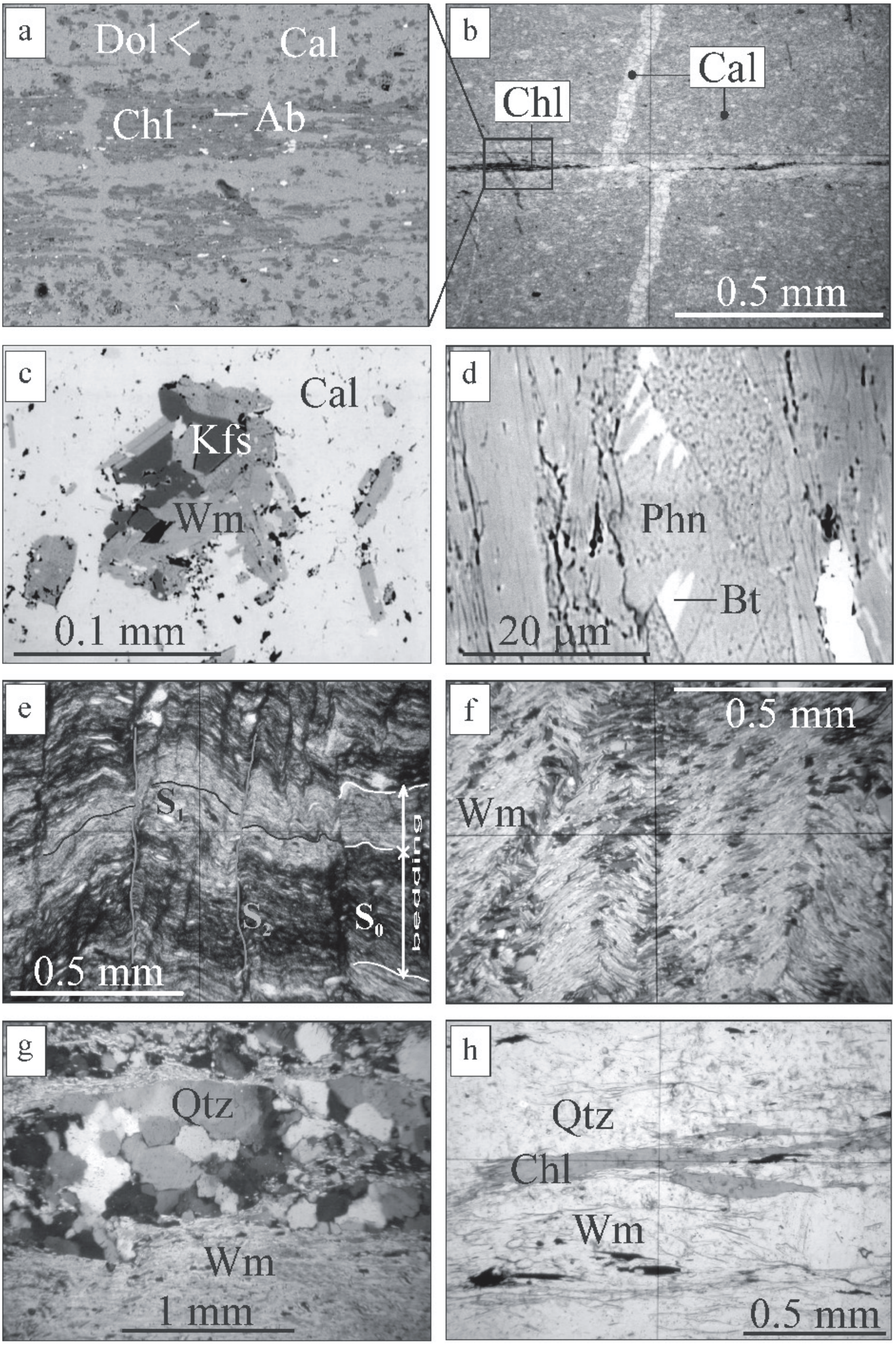
a
Dol
Cal
Chl
Ab
b
Cal
Chl
0.5 mm
c
Cal
Kfs
Wm
0.1 mm
d
Phn
Bt
20 μm
e
$S_1$
$S_2$
$S_0$
bedding
0.5 mm
f
0.5 mm
Wm
g
Qtz
Wm
1 mm
h
Qtz
Chl
Wm
0.5 mm

**Fig. 2.**

with respect to the foliation $S_1$, and pre- to syn-kinematic with respect to the ECC planes.

The Veľký Bok Unit exhibits imbricated fold-and-thrust structures developed during several deformation stages (Plašienka 1995). Thrust stacking occurred in front of the Veporic crustal wedge and in the rear of the detached Mesozoic sedimentary complexes which later became the Fatric Krížna cover nappe system (e.g. Plašienka et al. 1997).

## Petrography and deformational microtextures

The samples were collected from the central and marginal parts of the Veporic Superunit (Fig. 1). Representative lithological types (Fig. 2), namely Scythian metaquartzites, schists and Middle to Late Triassic marbles were investigated. Lithology, stratigraphic position and mineral assemblages of the collected samples are listed in Table 1.

Metaquartzites and related schists contain mainly white mica and quartz. K-feldspar and albite are present in various amounts and chlorite can be found only sporadically in a few samples. Tourmaline is the main accessory mineral.

Marbles are composed mainly of recrystallized calcite. Dolomite, albite, K-feldspar, quartz, white mica and chlorite are also present.

Metaquartzites are entirely recrystallized, showing strong preferred orientation of mica foliae. The detrital quartz grains are flattened and stretched with undulose extinction in the most deformed rocks. Grain size of recrystallized quartz in the mica-poor layers is larger than in the mica-rich layers, because in the latter, the grain growth was limited by mica grains pinning at the quartz grain boundaries. Some quartz porphyroclasts show shape-preferred orientation due to dissolution along boundaries parallel to foliation. The extent of the pressure solution has been enhanced in some cases by the presence of deformation resistant magnetite grains. Both the face and displacement controlled pyrite-type quartz fibres formed in the pressure shadows.

Marbles exhibit various grain size and microstructures. Foliation planes are defined by elongated coarse-grained relict calcite porphyroclasts and dynamically recrystallized fine-grained calcite matrix, both showing shape preferred orientation. For the first set of grains clockwise and anticlockwise twins are dominant. They become subparallel to the foliation with increasing strain intensity. Dolomite porphyroclasts behave as rigid bodies and are concentrated with other insoluble material on the zig-zag stylolitic boundaries. The authigenic white mica and chlorite concentrate in thin layers together with quartz, but they are also widespread as single flakes in the marble oriented subparallel to the main foliation plane (Lupták et al. 2001).

## Analytical methods

15 white K-mica-bearing samples of various lithologies and stratigraphic locations (Table 1) were prepared for X-ray powder diffraction following the procedures recommended by Kisch (1991). They were initially hammer-crushed followed by further, gentle disaggregation using a Sieb Mill for less than 30 s. Carbonate was removed by treatment with 5% acetic acid. Slides of oriented <2 μm fractions were prepared by a pipette method following the sedimentation of disaggregated samples in distilled water (Brindley & Brown 1984), keeping the specimen thickness of 5 mg/cm$^2$. Measurements were made using a Siemens D-5000 diffractometer (University Basel) at 40 kV, 30 mA and CuKα radiation. Air-dried sample mounts were scanned in the range of 2°–21° 2θ with a scanning rate of 0.03°2θ/20 s. Illite and chlorite "crystallinity" data (Kübler 1967, 1968; Frey 1987; Árkai 1991; Árkai et al. 1995; Warr 1996), i.e. the half-height width values of the first basal reflection of muscovite (Kübler index — KI) and the second basal reflection of chlorite (ChC) were calculated using the Siemens profile fitting package DIFFRACPlus: Profile plus v. 1.06. The KI values for the diagenetic zone/anchizone and the anchizone/epizone boundary are 0.42° and 0.25° Δ2θ CuKα, respectively (see Frey 1988; Dalla Torre & Frey 1997).

The chemical composition of selected minerals was obtained from polished thin sections by wavelength-dispersive

**Table 1:** Lithology, stratigraphy and mineral assemblages of the studied samples. Mineral abbreviations after Kretz (1983).

| Sample | Lithology | Stratigraphic position, unit | white mica | Chl | Qtz | Dol | Cal | Ab | Kfs | Kln | Tur | Bt | Ilm | Rt | Mag | Hem | KI | ChC |
|---|---|---|---|---|---|---|---|---|---|---|---|---|---|---|---|---|---|---|
| **DOPO1** | metaquartzite | Scythian, Foederata | x | o | x | | | x | x | o | x | | x | x | | | 0.22 | 0.25 |
| **DOPO2** | schist | Scythian, Foederata | x | o | x | x | | | x | | x | x | x | x | | | - | - |
| **DOPO4** | marble | Triassic, Foederata | x | o | x | x | x | | x | o | | | | | | | 0.25 | - |
| **DOPO13** | marble | Triassic, Foederata | x | | x | x | x | | x | | | | | | | | 0.23 | - |
| **MB3** | schist | Scythian, Foederata | x | | x | | | | x | o | x | | | | | | 0.19 | - |
| **RR1** | metaquartzite | Scythian, Foederata | x | | x | | | | | o | x | | | | x | | 0.26 | - |
| **TEL1** | schist | Scythian, Foederata | x | x | x | | | x | x | | | | x | | | | 0.17 | 0.15 |
| **TEL3** | metaquartzite | Scythian, Foederata | x | o | x | | | x | x | | x | | | | | | 0.25 | 0.25 |
| **TRE2** | schist | Scythian, Foederata | x | o | x | | | | | o | x | | | | x | | 0.26 | - |
| **ZB1** | schist | Scythian, Foederata | x | | x | | | | | | x | | x | | | | 0.21 | - |
| **ZB2** | schist | Scythian, Foederata | x | x | x | | | | x | o | x | | | | | | 0.23 | - |
| **ZE1** | schist | Scythian, Foederata | x | x | x | | | x | x | o | x | | x | x | | | 0.14 | - |
| **ZE4** | schist | Scythian, Foederata | x | | x | | | | x | | x | x | x | x | | | 0.26 | - |
| **LU6** | schist | Carpathian. Keuper Fm., VB | o | o | o | | | | | | | | | | | x | 0.29 | 0.22 |
| **LUC7** | marly limestone | Tithonian – Neocomian, VB | o | x | x | x | x | x | | | | | | | | | 0.30 | 0.22 |
| **VAL1** | schist | Carpathian. Keuper Fm., VB | x | x | x | | | x | | | | | | | | x | 0.27 | 0.22 |

VB — Veľký Bok; KI — "Kübler index", air-dried °Δ2θ CuKα; ChC — Chlorite "crystallinity" (002) AD °Δ2θ CuKα; AD — air dried; x — major phase recognized by microscopy; o — minor phase detected by X-ray.

spectroscopy method using a Jeol JXA-8600 electron-microprobe at the Institute of Mineralogy and Petrology, University of Basel. The operating conditions were set at an acceleration voltage of 15 kV and a 10 nA beam current. Natural and synthetic standards were used and the data were reduced by the PROZA routine.

## Results

### *Electron microprobe data*

Due to the fine grain size of samples studied by the X-ray diffraction method, microprobe data were obtained only on 11 samples. The compositions of authigenic white mica, chlorite, feldspar and biotite are presented below:

#### *White mica*

Representative analyses of white mica are shown in Table 2. Si ranging from 6.33 to 6.53 a.p.f.u. and Fe/(Fe+Mg) ratio of 0.46–0.74 are characteristic for the K-white micas in metaclastics. The K-white mica of the marble is characterized by 6.71 Si a.p.f.u. and Fe/(Fe+Mg) lower than 0.01. All K-white mica analyses from the investigated samples plot parallel to, but below the Tschermak exchange vector (Fig. 3). This indicates the presence of some ferrimuscovite component (Hunziker et al. 1986). The Na content is constantly low, the K content is more variable and the interlayer occupancy clusters around the theoretical mica value of 2.0 (Fig. 3). The sum of octahedral and interlayer cations shows a higher value than the theoretical one in some cases. This can be explained by the presence of noticeable $Fe^{3+}$ amount.

#### *Chlorite*

Mean analyses of authigenic-metamorphic chlorite are shown in Table 3. The chemical data were screened through a quality-control grid according to criteria proposed by Foster (1962) and Zane et al. (1998). The number of tetrahedral aluminium atoms is 2.32–2.75. The Si content of the chlorites is 5.25–5.68 a.p.f.u. and the Fe/(Fe+Mg) ratio ranges from 0.19 to 0.55. Mn and Ti contents are negligible.

#### *Biotite and feldspars*

Representative analyses of biotite are shown in Table 2. Ti contents up to 0.36 a.p.f.u. are characteristic for these biotites. The feldspars are albite and K-feldspar (Table 4).

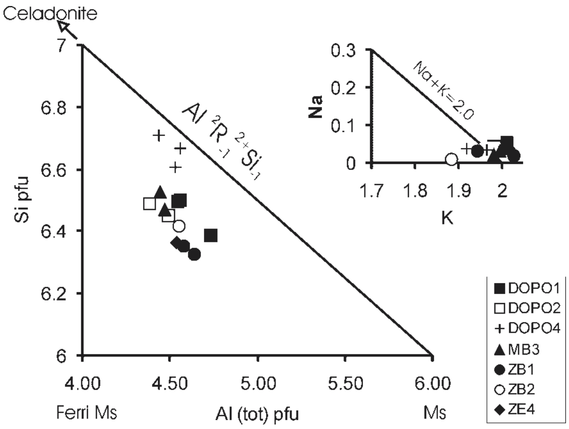

**Fig. 3.** Microprobe analyses of white K-micas plotted in Si-$Al^{tot}$ and Na-K diagrams.

**Table 2:** Representative chemical analyses of authigenic white mica and biotite. Formulae calculated on the basis of 22 oxygens.

| Sample analysis # | DOPO1 Phn2 | DOPO1 Phn3 | DOPO2 Phn1 | DOPO2 Phn3 | DOPO4 Phn2 | DOPO4 Phn3 | MB3 Phn2 | MB3 Phn3 | ZB1 Phn2 | ZB1 Phn6 | ZB2 Phn2 | ZE4 Phn3 | DOPO2 Bt5 | ZE4 Bt4 |
|---|---|---|---|---|---|---|---|---|---|---|---|---|---|---|
| **$SiO_2$** | 47.58 | 47.89 | 47.21 | 47.23 | 50.35 | 50.88 | 47.94 | 47.76 | 45.67 | 44.99 | 46.39 | 45.74 | 36.32 | 36.47 |
| **$Al_2O_3$** | 28.31 | 28.44 | 27.03 | 27.91 | 29.28 | 28.56 | 28.10 | 27.59 | 28.40 | 27.53 | 27.89 | 27.66 | 15.90 | 17.48 |
| **$TiO_2$** | 0.88 | 0.80 | 1.14 | 1.26 | 0.96 | 0.21 | 1.31 | 0.69 | 1.01 | 1.23 | 0.98 | 0.98 | 3.03 | 3.11 |
| **MgO** | 2.46 | 2.62 | 2.23 | 2.05 | 3.97 | 4.37 | 2.00 | 1.93 | 1.59 | 1.39 | 1.76 | 2.18 | 9.97 | 10.14 |
| **FeO** | 4.00 | 4.00 | 6.47 | 5.83 | 0.03 | 0.07 | 6.12 | 6.39 | 7.48 | 7.18 | 7.10 | 6.68 | 19.04 | 17.16 |
| **MnO** | 0.00 | 0.01 | 0.00 | 0.03 | 0.00 | 0.00 | 0.00 | 0.02 | 0.00 | 0.01 | 0.03 | 0.03 | 0.14 | 0.06 |
| **CaO** | 0.01 | 0.04 | 0.00 | 0.00 | 0.11 | 0.10 | 0.00 | 0.02 | 0.02 | 0.00 | 0.01 | 0.01 | 0.00 | 0.01 |
| **$Na_2O$** | 0.14 | 0.20 | 0.16 | 0.16 | 0.15 | 0.13 | 0.08 | 0.12 | 0.11 | 0.07 | 0.03 | 0.14 | 0.05 | 0.05 |
| **$K_2O$** | 11.52 | 11.62 | 11.31 | 11.39 | 11.79 | 11.68 | 11.52 | 11.46 | 11.00 | 11.26 | 10.68 | 11.37 | 10.15 | 9.18 |
| **Total** | 94.89 | 95.62 | 95.55 | 95.85 | 96.64 | 96.00 | 97.07 | 95.98 | 95.28 | 93.66 | 94.88 | 94.79 | 94.59 | 93.65 |
| **Si** | 6.50 | 6.50 | 6.49 | 6.45 | 6.61 | 6.71 | 6.47 | 6.53 | 6.33 | 6.35 | 6.42 | 6.36 | 5.60 | 5.57 |
| **$Al^{iv}$** | 1.50 | 1.50 | 1.51 | 1.55 | 1.39 | 1.29 | 1.53 | 1.48 | 1.68 | 1.65 | 1.58 | 1.64 | 2.40 | 2.43 |
| **$Al^{vi}$** | 3.06 | 3.05 | 2.87 | 2.94 | 3.14 | 3.15 | 2.94 | 2.97 | 2.96 | 2.93 | 2.97 | 2.90 | 0.49 | 0.72 |
| **Ti** | 0.09 | 0.08 | 0.12 | 0.13 | 0.10 | 0.02 | 0.13 | 0.07 | 0.11 | 0.13 | 0.10 | 0.10 | 0.35 | 0.36 |
| **Mg** | 0.50 | 0.53 | 0.46 | 0.42 | 0.78 | 0.86 | 0.40 | 0.39 | 0.33 | 0.29 | 0.36 | 0.45 | 2.29 | 2.31 |
| **$Fe^{2+}$** | 0.46 | 0.45 | 0.74 | 0.67 | 0.00 | 0.01 | 0.69 | 0.73 | 0.87 | 0.85 | 0.82 | 0.78 | 2.45 | 2.19 |
| **Mn** | 0.00 | 0.00 | 0.00 | 0.00 | 0.00 | 0.00 | 0.00 | 0.00 | 0.00 | 0.00 | 0.00 | 0.00 | 0.02 | 0.01 |
| **Ca** | 0.00 | 0.01 | 0.00 | 0.00 | 0.02 | 0.01 | 0.00 | 0.00 | 0.00 | 0.00 | 0.00 | 0.00 | 0.00 | 0.00 |
| **Na** | 0.04 | 0.05 | 0.04 | 0.04 | 0.04 | 0.03 | 0.02 | 0.03 | 0.03 | 0.02 | 0.01 | 0.04 | 0.02 | 0.02 |
| **K** | 2.01 | 2.01 | 1.98 | 1.99 | 1.98 | 1.97 | 1.98 | 2.00 | 1.94 | 2.03 | 1.89 | 2.02 | 2.00 | 1.79 |
| **Fe/(Fe+Mg)** | 0.48 | 0.46 | 0.62 | 0.62 | 0.00 | 0.01 | 0.63 | 0.65 | 0.73 | 0.74 | 0.69 | 0.63 | 0.52 | 0.49 |
| **X(Ca)** | 0.000 | 0.003 | 0.000 | 0.000 | 0.007 | 0.007 | 0.000 | 0.001 | 0.002 | 0.000 | 0.001 | 0.000 | 0.000 | 0.001 |
| **X(Na)** | 0.018 | 0.026 | 0.021 | 0.021 | 0.019 | 0.016 | 0.010 | 0.016 | 0.015 | 0.009 | 0.004 | 0.018 | 0.007 | 0.008 |
| **X(K)** | 0.981 | 0.971 | 0.979 | 0.979 | 0.974 | 0.977 | 0.990 | 0.983 | 0.983 | 0.991 | 0.995 | 0.981 | 0.993 | 0.991 |

**Table 3:** Mean chemical analyses of authigenic chlorites. Formulae calculated on the basis of 28 oxygens, assuming all Fe as $Fe^{2+}$.

| Sample<br>analysis # | LUC7<br>(n = 8) | VAL1<br>(n = 5) | TEL1<br>(n = 7) | ZE1<br>(n = 9) |
|---|---|---|---|---|
| $SiO_2$ | 27.00 | 28.61 | 27.98 | 25.30 |
| $Al_2O_3$ | 22.06 | 22.72 | 22.53 | 22.71 |
| $TiO_2$ | 0.07 | 0.12 | 0.03 | 0.06 |
| MgO | 12.05 | 25.12 | 24.91 | 16.99 |
| FeO | 25.94 | 10.42 | 10.45 | 22.06 |
| MnO | 0.27 | 0.04 | 0.45 | 0.21 |
| CaO | 0.02 | 0.00 | 0.00 | 0.01 |
| $Na_2O$ | 0.01 | 0.00 | 0.00 | 0.01 |
| $K_2O$ | 0.23 | 0.08 | 0.02 | 0.04 |
| Total | 87.64 | 87.10 | 86.39 | 87.39 |
| | | | | |
| Si | 5.68 | 5.57 | 5.51 | 5.25 |
| $Al^{iv}$ | 2.32 | 2.43 | 2.49 | 2.75 |
| $Al^{vi}$ | 3.14 | 2.79 | 2.74 | 2.81 |
| Ti | 0.01 | 0.02 | 0.01 | 0.01 |
| Mg | 3.77 | 7.29 | 7.32 | 5.26 |
| $Fe^{2+}$ | 4.56 | 1.70 | 1.72 | 3.83 |
| Mn | 0.05 | 0.01 | 0.08 | 0.04 |
| Ca | 0.01 | 0.00 | 0.00 | 0.00 |
| Na | 0.00 | 0.00 | 0.00 | 0.00 |
| K | 0.06 | 0.02 | 0.01 | 0.01 |
| | | | | |
| Fe/(Fe+Mg) | 0.55 | 0.19 | 0.19 | 0.42 |
| T(°C) | 312±30 | 329±8 | 340±8 | 380±10 |
| T(°C)* | 319±30 | 325±8 | 335±8 | 382±10 |

T(°C) — Cathelineau (1988); T(°C)* — Jowett (1991)

**Table 4:** Representative chemical analyses of authigenic feldspars. Formulae calculated on the basis of 8 oxygens.

| Sample<br>analysis # | DOPO2<br>Kfs1 | DOPO4<br>Kfs4 | MB3<br>Kfs10 | ZB2<br>Kfs1 | ZE4<br>Kfs1 | LUC7<br>Ab7 |
|---|---|---|---|---|---|---|
| $SiO_2$ | 64.67 | 63.60 | 63.04 | 62.79 | 62.46 | 67.57 |
| $Al_2O_3$ | 18.14 | 18.38 | 19.04 | 19.29 | 18.77 | 21.18 |
| $TiO_2$ | 0.03 | 0.00 | 0.00 | 0.00 | 0.00 | 0.00 |
| MgO | 0.01 | 0.01 | 0.00 | 0.00 | 0.01 | 0.41 |
| FeO | 0.00 | 0.00 | 0.03 | 0.15 | 0.13 | 0.38 |
| MnO | 0.08 | 0.00 | 0.00 | 0.00 | 0.00 | 0.03 |
| CaO | 0.00 | 0.16 | 0.00 | 0.02 | 0.00 | 0.21 |
| $Na_2O$ | 0.78 | 0.26 | 0.78 | 0.60 | 0.80 | 8.26 |
| $K_2O$ | 17.03 | 17.40 | 17.02 | 16.57 | 17.04 | 0.21 |
| Total | 100.74 | 99.82 | 99.91 | 99.42 | 99.21 | 98.25 |
| | | | | | | |
| Si | 2.99 | 2.97 | 2.94 | 2.94 | 2.94 | 2.97 |
| Al | 0.99 | 1.01 | 1.05 | 1.06 | 1.04 | 1.10 |
| Ti | 0.00 | 0.00 | 0.00 | 0.00 | 0.00 | 0.00 |
| Mg | 0.00 | 0.00 | 0.00 | 0.00 | 0.00 | 0.03 |
| $Fe^{2+}$ | 0.00 | 0.00 | 0.00 | 0.01 | 0.01 | 0.01 |
| Mn | 0.00 | 0.00 | 0.00 | 0.00 | 0.00 | 0.00 |
| Ca | 0.00 | 0.01 | 0.00 | 0.00 | 0.00 | 0.01 |
| Na | 0.07 | 0.02 | 0.07 | 0.05 | 0.07 | 0.70 |
| K | 1.00 | 1.04 | 1.01 | 0.99 | 1.02 | 0.01 |
| | | | | | | |
| An | 0.000 | 0.007 | 0.000 | 0.001 | 0.000 | 0.014 |
| Ab | 0.065 | 0.022 | 0.065 | 0.052 | 0.067 | 0.970 |
| Or | 0.935 | 0.970 | 0.935 | 0.947 | 0.933 | 0.017 |

### *X-ray diffraction of the < 2 μm fraction*

X-ray powder diffraction patterns of oriented <2 μm fraction show that illite-muscovite and chlorite±quartz, albite and K-feldspar are the main phases present. Sample TEL1 contains a subordinate amount of paragonite. Calibrated KI and ChC values have been used to determine relative changes in metamorphic grade (see the part "Analytical methods"). The calibrated values for the studied samples are presented in Table 1. The KI data range from 0.14 to 0.30 °Δ2θ and ChC from 0.15 to 0.25 °Δ2θ. Representative diffractograms from various lithologies (Fig. 4) illustrate decreasing KI with increasing metamorphic grade. Figure 5 shows the difference and variation of KI from the western to the eastern part of the Veporic Superunit.

The relationship between the chemistry and KI values of micas has been discussed by Árkai et al. (2002). They found a correlation between the KI and celadonite content of white K-

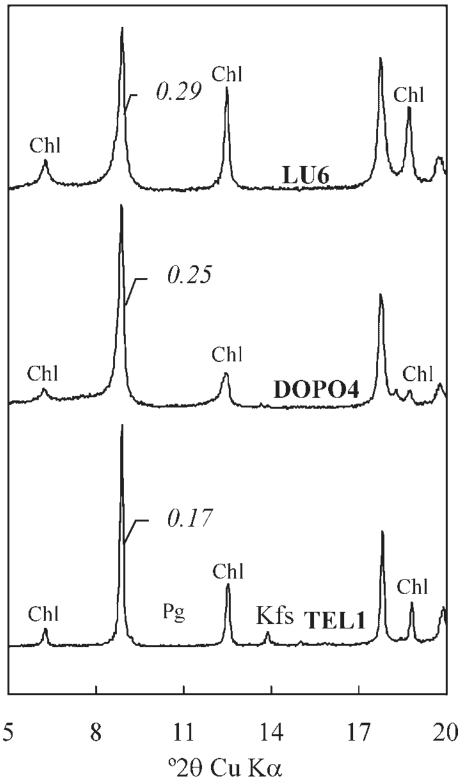

**Fig. 4.** Diffractograms of some illite-muscovite-rich clay fractions showing the first two basal reflections. Samples are arranged with increasing (downwards) metamorphic grade according to their illite "crystallinity" values. Impurities include chlorite, quartz and K-feldspar (TEL1).

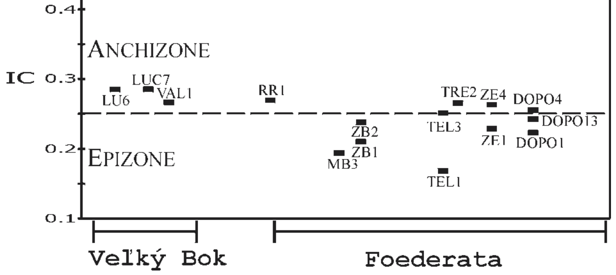

**Fig. 5.** KI variation in the investigated metasediments from the western to the eastern part of the Veporic Superunit.

mica. Increasing Si content (Fig. 6a) and decreasing $Al^{iv}/(Al^{iv}+Fe^{2+}+Mg)$ ratio (Fig. 6b) of white K-mica with increasing KI were also observed in samples from the Foederata Unit.

### *Thermobarometry*

To determine the temperature conditions, the chlorite thermometer of Cathelineau (1988) based on $Al^{iv}$ substitution in chlorites was used, together with its modified version by Jowett (1991). Both thermometers gave only slightly different results, showing an increase in temperature from ca. 310 to 380 °C (Table 3). Lower (~310–330 °C) temperatures were obtained from chlorites of the Veľký Bok Unit compared to those from the Foederata Unit (~335–380 °C). Although the chlorite thermometry is mostly inaccurate in sedimentary rocks (e.g. Schmidt et al. 1997), since it was calibrated for volcanic rocks (Cathelineau 1988), the increasing trend of metamorphic temperatures in the studied units is obvious and corresponds with the obtained phyllosilicate "crystallinity" data.

In the easternmost part of the Foederata Unit, pressure was estimated in the K-feldspar and biotite-bearing schists from the reaction: 3Cel = Phl + 2Kfs + 3Qtz + $2H_2O$ (Fig. 7), using the computer program THERMOCALC v. 3.1 (Powell & Holland 1988) and the internally consistent thermodynamic dataset of Holland & Powell (1998). A pressure of ca. 4–4.5 kbar at a temperature of ~380 °C was obtained from the intersection with the chlorite geothermometer (Fig. 7).

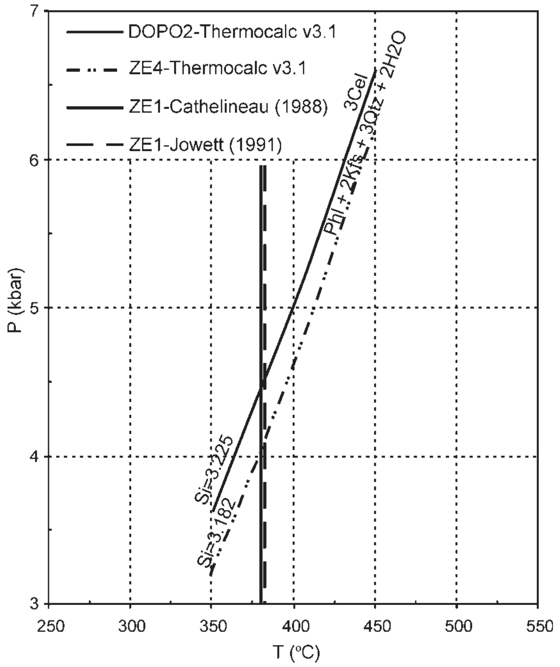

**Fig. 7.** Pressure and temperature conditions calculated from the reaction 3Cel = Phl + 2Kfs + 3Qtz a $2H_2O$ with thermodynamic data of Holland & Powell (1998) and chlorite thermometry (Cathelineau 1988; Jowett 1991).

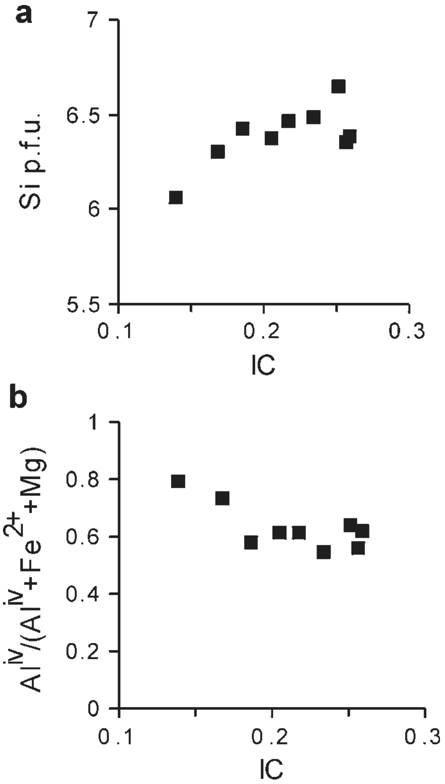

**Fig. 6.** Relations between KI of white K-micas and their chemical compositions from the Foederata Unit. Electron microprobe data used in diagrams represent average chemical analyses of white K-mica (n — number of analyses). Samples (from bottom-left to top-right): ZE1 (n = 3), TEL1 (n = 7), MB3 (n = 6), ZB1 (n = 6), DOPO1 (n = 3), ZB2 (n = 3), DOPO4 (n = 4), TRE2 (n = 3), ZE4 (n = 4).

## Discussion

In general, the illite "crystallinity" method has been used mainly to set the beginning of metamorphism. Its accuracy decreases from the anchizone towards either diagenesis or epizone (Kübler & Jaboyedoff 2000). The effect of the detrital micas and illite-smectite on the KI decreases with burial and disappears almost completely in the anchizone (Kübler & Jaboyedoff 2000).

The presented KI data point to metamorphic conditions of the upper anchizone (samples from the Veľký Bok Unit), but most of the samples (Foederata Unit) belong to the anchizone/epizone transition and epizone.

Plašienka et al. (1989) estimated the temperature of Alpine metamorphism at ca. 350 °C in the Veporic cover rocks. By contrast, Korikovsky et al. (1992) obtained lower temperatures ranging between ca. 200 and 300 °C. Our KI and chlorite thermometry results together with microtextural observations suggest higher metamorphic temperatures than the previous estimates. Pressure conditions obtained by Mazzoli et al. (1992) from the $b_0$ spacing in K-white micas gave up to 12 kbar and Korikovsky et al. (1997) assumed 8–9 kbar from the phengite barometer of Massone & Schreyer (1987). This study, however, suggests that pressure during the Alpine low-grade metamorphism (at ca. 380 °C) was probably not so high, not exceeding ca. 4.5 kbar in the cover metasediments.

Higher, amphibolite facies conditions of Alpine metamorphism (up to 620 °C and 10 kbar) were reached in the deeper tectonic units of the Veporic core complex (Lupták et al. 2000; Janák et al. 2001), suggesting a metamorphic gradient of ca. 15 °C/km.

## Conclusions

Our results suggest that the studied metasedimentary rocks in the Veporic Superunit were metamorphosed in upper anchizonal to epizonal (greenschist facies) conditions. The temperature ranges from approximately 310–330 °C in the northwestern parts of the Veporic cover, including the Veľký Bok Unit, up to approximately 335–380 °C in the central and eastern parts (Foederata Unit). The estimated pressure conditions reached about 4.5 kbar. Alpine metamorphism caused complete recrystallization of former clay minerals and the growth of newly formed white mica, chlorite and feldspars. These data suggest that the Alpine regional metamorphic grade increased from the Mesozoic cover to the underlying Late Paleozoic and basement rocks in the Veporic Superunit, which is consistent with a metamorphic core complex structure and the Cretaceous tectonometamorphic evolution of this area outlined by Plašienka et al. (1999); Lupták et al. (1999, 2000) and Janák et al. (2001).

**Acknowledgments:** This work is dedicated to late Martin Frey who encouraged and supported new studies on Alpine metamorphism in the Western Carpathians. We thank W.B. Stern (Basel) for his help with X-ray measurements. The first manuscript greatly benefited from the critical remarks by R. Ferreiro Mählmann. Reviews by P. Árkai, A. Vozárová and C. Mazzoli further clarified the paper and are greatly appreciated. The research has been financially supported by the Slovak Grant Agency for Science (Project No. 3167) and the Slovak Agency for Support of Science and Technology APVT (Project No. 20-020002) which is gratefully acknowledged.

## References

Árkai P. 1991: Chlorite crystallinity: an empirical approach and correlation with illite crystallinity, coal rank and mineral facies as exemplified by Palaeozoic and Mesozoic rocks of northwest Hungary. *J. Metamorph. Geology* 9, 723–734.

Árkai P., Sassi F.P. & Sassi R. 1995: Simultaneous measurements of chlorite and illite crystallinity: a more reliable geothermometric tool for monitoring low- to very low-grade metamorphism in metapelites. A case study from Southern Alps (NE Italy). *Eur. J. Mineral.* 7, 1115–1128.

Árkai P., Fenninger A. & Nagy G. 2002: Effects of lithology and bulk chemistry on phyllosilicate reaction progress in the low-T metamorphic Graz Paleozoic, Eastern Alps, Austria. *Eur. J. Mineral.* 14, 673–686.

Biely A. 1989: The geological structure of the West Carpathians. In: Rakús M., Dercourt J. & Nairn A.E.M. (Eds.): Evolution of the northern margin of Tethys. *Mém. Soc. Géol. France,* Nouvelle Série No. 154 (II), 51–57.

Brindley G.W. & Brown G. 1984: Crystal structures of clay minerals and their X-ray identification. *Mineral. Soc. London.*

Cathelineau M. 1988: Cation site occupancy in chlorites and illites as a function of temperature. *Clay Miner.* 23, 471–485.

Dalla Torre M. & Frey M. 1997: The evolution from disordered Ad to ordered $2M_1$ white K-mica polytype in low-temperature metamorphosed sedimentary rocks. *Schweiz. Mineral. Petrogr. Mitt.* 77, 149–159.

Foster M.D. 1962: Interpretation of the composition and a classification of the chlorites. *U.S. Geol. Surv., Prof. Pap.* 414A, 1–33.

Frey M. 1987: Very low-grade metamorphism of clastic sedimentary rocks. In: Frey M. (Ed.): Low temperature metamorphism. *Blackie & Son,* Glasgow, 9–58.

Frey M. 1988: Discontinuous inverse metamorphic zonation, Glarus Alps, Switzerland: evidence from illite "crystallinity" data. *Schweiz. Mineral. Petrogr. Mitt.* 68, 171–183.

Holland T.J.B. & Powell R. 1998: An internally consistent thermodynamic data set for phases of petrological interest. *J. Metamorph. Geology* 16, 309–343.

Hunziker J.C., Frey M., Clauer N., Dallmeyer R.D., Friedrichsen H., Flehmig W., Hochstrasser K., Roggwiler P. & Schwander H. 1986: The evolution of illite to muscovite: mineralogical and isotopic data from the Glarus Alps, Switzerland. *Contr. Mineral. Petrology* 92, 157–180.

Janák M., Plašienka D., Frey M., Cosca M., Schmidt S.Th., Lupták B. & Méres Š. 2001: Cretaceous evolution of a metamorphic core complex, the Veporic unit, Western Carpathians (Slovakia): P-T conditions and in situ $^{40}$Ar/ $^{39}$Ar UV laser probe dating of metapelites. *J. Metamorph. Geology* 19, 197–216.

Jowett E.C. 1991: Fitting iron and magnesium into the hydrothermal chlorite geothermometer. *Geol. Assoc. Canada/ Mineral. Assoc. Canada/ Soc. Econ. Geol. Joint Annual Meeting,* Toronto, Program with Abstracts 16, A62.

Kisch H.J. 1991: Illite crystallinity: recommendations on sample preparation, X-ray diffraction settings, and interlaboratory samples. *J. Metamorph. Geology* 9, 665–670.

Korikovsky S.P., Putiš M. & Boronikhin V.A. 1992: Anchimetamorphism of Permian sandstones of the Struženík group in the Nízke Tatry Mts. (Western Carpathians). *Geol. Carpathica* 43, 2, 97–104.

Korikovsky S.P., Putiš M. & Plašienka D. 1997: Cretaceous low-grade metamorphism of the Veporic and North-Gemeric Zones: a result of collisional tectonics in the central Western Carpathians. In: Grecula P., Hovorka D. & Putiš M. (Eds.): Geological evolution of the Western Carpathians. *Miner. Slovaca-Monograph, Geocomplex,* Bratislava, 107–130.

Kretz R. 1983: Symbols for rock-forming minerals. *Amer. Mineralogist* 68, 277–279.

Kübler B. 1967: La cristallinité de l´illite et les zones tout à fait supérieures du métamorphisme. *Etages tectoniques. Colloque de Neuchâtel,* 105–122.

Kübler B. 1968: Evaluation quantitative du métamorphisme par la cristallinité de l´illite. *Bull. Cent. Rech. Pau* SNPA 2, 385–397.

Kübler B. & Jaboyedoff M. 2000: Illite crystallinity. *Earth Planet. Sci.* 331, 75–89.

Lupták B., Frey M., Janák M., Schmidt S.Th. & Plašienka D. 1999: Alpine metamorphism of the Mesozoic cover rocks from the Veporic unit, Western Carpathians: X-ray and EMP study of white mica and chlorite. *Geol. Carpathica* Spec. Issue, 50, 122–123.

Lupták B., Janák M., Plašienka D., Schmidt S.Th. & Frey M. 2000: Chloritoid-kyanite schists from the Veporic unit, Western Carpathians, Slovakia: implications for Alpine (Cretaceous) metamorphism. *Schweiz. Mineral. Petrogr. Mitt.* 80, 211–222.

Lupták B., Plašienka D., Janák M. & Vojtko R. 2001: Development of deformational structures during Alpine metamorphism of the Mesozoic cover rocks in the Veporic unit, Western Carpathians. *Geol. Paläont. Mitt.* 25, 136–137.

Massonne H. & Schreyer W. 1987: Phengite geobarometry based on the limiting assemblage with K-Feldspar, Phlogopite and Quartz. *Contr. Mineral. Petrology* 96, 212–224.

Mazzoli C., Sassi R. & Vozárová A. 1992: The pressure character of the Alpine metamorphism in the Central and Inner Western Carpathians (Czecho-Slovakia). In: Vozár J. (Ed.): The Alpine geodynamic domains: Western Carpathians, Eastern Alps, Dinarides. *Conf. Symp.Sem., D. Štúr. Inst. Geol.,* Bratislava, 109–117.

Plašienka D. 1995: Cleavages and folds in changing tectonic regimes: the Veľký Bok Mesozoic cover unit of the Veporicum (Nízke Tatry Mts., Central Western Carpathians). *Slovak Geol. Mag.* 2, 97–113.

Plašienka D., Janák M., Hacura A. & Vrbatovič P. 1989: First illite crystallinity data from the Alpine metamorphosed rocks of the Veporicum. *Miner. Slovaca* 21, 43–51.

Plašienka D., Grecula P., Putiš M., Hovorka D. & Kováč M. 1997: Evolution and structure of the Western Carpathians: an overview. In: Grecula P., Hovorka D. & Putiš M. (Eds.): Geological evolution of the Western Carpathians. *Miner. Slovaca — Monograph, Geocomplex,* Bratislava, 107–130.

Plašienka D., Janák M., Lupták B., Milovský R. & Frey M. 1999: Kinematics and metamorphism of a Cretaceous core complex: the Veporic unit of the Western Carpathians. *Phys. Chem. Earth* (A) 24, 651–658.

Powell R. & Holland T.J.B. 1988: An internally consistent thermodynamic dataset with uncertainties and correlations: 3. Application to geobarometry worked examples and a computer program. *J. Metamorph. Geology* 6, 173–204.

Schmidt D., Schmidt S.Th., Mullis J., Ferreiro Mählmann R. & Frey M. 1997: Very low-grade metamorphism of the Taveyanne formation of western Switzerland. *Contr. Mineral. Petrology* 129, 385–403.

Tomek Č. 1993: Deep crustal structure beneath the central and inner West Carpathians. *Tectonophysics* 226, 417–431.

Vozárová A. & Vozár. J. 1988: Late Paleozoic in West Carpathians. *GÚDŠ,* Bratislava, 1–314.

Vrána S. 1966: Alpidische Metamorphose der Granitoide und Foederata-Serie im Mittelteil der Veporiden. *Zbor. Geol. Vied, Západ. Karpaty* 6, 29–84.

Warr L.N. 1996: Standardized clay mineral crystallinity data from the very low-grade metamorphic facies rocks of southern New Zealand. *Eur. J. Mineral.* 8, 115–127.

Zane A., Sassi R. & Guidotti Ch.V. 1998: New data on metamorphic chlorite as a petrogenetic indicator mineral, with special regard to greenschist-facies rocks. *Canad. Mineralogist* 36, 713–726.

## Appendix

Localities and samples description.

| Locality | Sample | Description |
|---|---|---|
| ***Foederata Unit*** | | |
| *DOBŠINÁ BROOK VALLEY* | | *west of Dobšiná town behind the Vyšná Maša (Foederata) settlement* |
| (DOPO) | DOPO1 | fine-grained metaquartzite |
| | DOPO2 | micaceous intercalation (shist) within metaquartzite |
| | DOPO4 | banded (grey and pinkish layers) marble (Wetterstein type) |
| | DOPO13 | grey marble (Reifling type) |
| *MALÁ BÔROVÁ MASSIVE* | | *southern slope of the Malá Bôrová massive NW from the Klenovec town* |
| (MB) | MB3 | micaceous intercalation (schist) within fine-grained metaquartzite |
| *RUŽINÁ DAM* | | *eastern margin of the water dam near its vent* |
| (RR) | RR1 | micaceous metaquartzite |
| *TELGÁRT* | | *north of Telgárt, ca. 1100 m above sea level* |
| (TEL) | TEL1 | white mica, chlorite, quartz and plagioclase (± K-feldspar) schist |
| | TEL3 | fine-grained metaquartzite |
| *TRESTNÍK MASSIVE* | | *quarry located NE from the Tresník hill* |
| (TRE) | TRE2 | micaceous intercalation (schist) within metaquartzite |
| *ZBOJSKÁ SADDLE* | | *quarry in the saddle Zbojská (road from Brezno to Tisovec)* |
| (ZB) | ZB1 | micaceous greenish intercalation (schist) within metaquartzite |
| | ZB2 | white mica, chlorite, quartz and K-feldspar schist |
| *ZELINOVÁ VALLEY* | | *Zelinova valley (SW of Rejdová village)* |
| (ZE) | ZE1 | white mica, chlorite, quartz and plagioclase (± K-feldspar) schist |
| | ZE4 | fine-grained micaceous intercalation (schist) in metaquartzite |
| ***Veľký Bok Unit (Lučatín Unit)*** | | |
| *ĽUBIETOVÁ and LUČATÍN* | | *Vôdka valley and the road between Ľubietová and Lučatín villages* |
| (LU and LUC) | LU6 | fine-grained violet schist (Carpathian Keuper Fm.) |
| | LUC7 | metamorphosed micritic marly limestone |
| *VALASKÁ VILLAGE* | | *rock cliff above a dead arm of the Hron river (road from Valaská to Brezno)* |
| (VAL) | VAL1 | fine-grained violet schist (Carpathian Keuper Fm.) |